J Solid State Electrochem (1997) 1: 241–247

ORIGINAL PAPER

Hong Shen · James E. Mark · Carl J. Seliskar
Harry B. Mark Jr. · William R. Heineman

Stripping voltammetry of copper and lead using gold electrodes modified with self-assembled monolayers

Received: 29 May 1997 / Accepted: 24 June 1997

Abstract One problem associated with using bare solid metal electrodes, such as gold and platinum, in stripping analysis to determine heavy metal ions such as lead and copper ions in dilute solutions is that underpotential deposition (UPD) gives multiple stripping peaks in the analysis of mixtures. These peaks are often overlapped and cannot be conveniently used for analytical purposes. Bifunctional alkylthiols, such as 3-mercaptopropionic acid, with an ionizable group on the other terminal end of the thiol can form self-assembled monolayers (SAMs) on the surface of the gold electrode. It is shown that such an SAM-modified gold electrode minimizes the UPD effects for the stripping analysis of lead and copper. The anodic peak potential shifts and the peak shape changes, indicating that the SAM changes the deposition and stripping steps of these heavy metal ions. Thus, the sensitivity levels for both single species and mixtures can be significantly improved for the conventional solid electrodes. The mechanism of the deposition reaction at the SAM-modified gold electrodes is discussed.

Key words Underpotential deposition · Stripping analysis · Self-assembled monolayers · Multiple stripping peaks · Heavy metals

Introduction

The design of electrodes with controllable surface properties continues to be a major area of research in recent years. One promising avenue to obtain higher selectivity for electrochemical detection is to cover the surface with an appropriate permselective coating [1–3]. Such surface barriers effectively exclude undesired interfering species from the electrode surface while allowing transport of the analyte. A large variety of discriminative coatings have been suggested for this purpose, including size-selective cellulose acetate [4, 5], poly(1,2-diaminobenzene) [6], charge-selective Nafion [7, 8], Eastman AQ [9], poly(vinylpyridine) [10] and hydrophobic lipid [11] layers. The monolayer self-assembly technique could yield a very simple, and yet highly versatile, controllable and stable approach for tailoring electrode surfaces. The well-defined SAM films have already proven to be extremely useful for studying ion binding [12–16], for incorporating redox couples into electrochemical interfaces [14, 15], for studying protein adsorption [13, 17], and for blocking electron transfer between redox species and electrode surfaces [18–20].

Ionic recognition and ionic pairing to achieve selective response in self-assembled monolayer films have also been of interest. Attempts have been made to create artificial supermolecular structures [21–30] to form monolayer membranes that selectively recognize a specific component in the presence of others. In this respect, gold electrodes modified with thioctic acid have been used to determine $Fe(CN)_6^{3-}$ and $Ru(NH_3)_6^{3+}$ at different pH values and in different supporting electrolytes [31]. The results were used to determine the packing quality and stability of the monolayers. Yip [32] and co-workers used *n*-mercaptoalkyl tetrathiafulvalenecarboxylate-modified gold electrodes to study the charge transfer between the monolayer and surrounding species. Sun [33] and co-workers developed a pH-dependent sensor that used a 4-aminothiophenol (4-ATP)-modified gold electrode to detect anthraquinone-2,6-disulfonate ($2,6\text{-}AQDS^{2-}$) electrochemically. Molecular recognition is best implemented by creating sites that exhibit both physical and chemical interactions with the target analyte [34, 35]. Many sensor designs involving SAMs only employ the simplest interaction, which is the electrostatic attraction between the

H. Shen · J.E. Mark · C.J. Seliskar · H.B. Mark Jr.
W.R. Heineman (✉)
Department of Chemistry, University of Cincinnati,
P.O. Box 210172, Cincinnati, OH 45221-0172, USA

monolayer and the analyte [36, 37]. Steinberg [30] used a unique ligand, 2,2′-thiobis(ethyl acetoacetate) (TBEA), to detect trace amounts of Cu^{2+} (down to 10^{-7} M) and Pb^{2+} (down to 10^{-5} M) in the presence of Fe^{2+} as an interference. The Fe^{2+} concentrations are about 100 to 10000 times higher than those of the analytes. This takes advantage of selective complexation between the ligand and the Cu^{2+} and Pb^{2+}. They noted that, during the stripping analysis of these metal ions [37], the UPD peaks were occasionally minimized by the SAM attached to the electrode surface.

The technique of stripping analysis [38] is a very sensitive electroanalytical technique. The method consists of two steps. The first one is a preconcentration step where a small portion of the unknown electroactive material is electrodeposited at the electrode surface under controlled conditions of mass transport. The second step involves the electrodissolution, or stripping, of the deposit. The technique has been most useful in the determination of trace levels of certain heavy metal ions in solution. In most of these applications the mercury film electrode [39] or the hanging mercury drop electrode [40, 41] has been used. These electrodes have been applicable where amalgam formation is involved. Unfortunately, whenever solid electrodes are used for the determination of other metal ions the UPD effects become a major problem. Multiple-peak curves are obtained at lower concentrations as shown by Nicholson [42, 43] in studies of the stripping of micro-deposits of nickel from platinum electrodes. Other investigators [44, 45] concluded that the activities of these deposits could vary with the extent of surface and crystal lattice sites of the electrode. They concluded that bonding forces between the electrode and the deposit of the first monolayer could be stronger than those between the like atoms of the deposit of subsequent layers. Also, some portions of the monolayer deposit could be bonded with different energies at different electrode surface lattice sites. This makes quantitative analysis of dilute solutions virtually impossible.

The objective in this paper is to use bifunctional thiols to form an SAM on the gold electrode surface to prevent the UPD effects in the stripping analysis of heavy metal ions.

Experimental

Materials

Bifunctional 3-mercaptopropionic acid was purchased from Aldrich Chemicals (Milwaukee, Wis.). Concentrated sulfuric acid, lead nitrate, and copper nitrate were purchased from Fisher Scientific (Fair Lawn, N.J.). Absolute ethanol was obtained from Aaper Alcohol and Chemical (Shelbyville, Ky.). All reagents were of analytical grade. Gold disk electrodes (surface area $A = 2.01$ mm^2) were obtained from Bioanalytical Systems (West Lafayette, Ind.) and Fibrmet polishing disks (Buehler, Lake Bluff, Ill.) were used to polish the electrode surface. Water was purified with a Barnstead organic pure water system.

Apparatus

Cyclic voltammetry (CV), linear sweep voltammetry (LSV), linear sweep stripping voltammetry (LSSV), and Osteryoung square wave stripping voltammetry (OSWSV) experiments were carried out with a BAS-100B/W System. The electrochemical cell consisted of a BAS Ag/AgCl, 3 M NaCl reference electrode, a platinum auxiliary electrode and a bare or an SAM-modified gold working electrode.

SAM solution preparation

All SAM solutions were prepared by dissolving the thiol in absolute ethanol at room temperature.

Electrode preparation

The gold electrodes were first polished on a 3-μm silicon carbide disk followed by a 0.3-μm aluminum oxide disk. The polished electrodes were then dipped into Piranha solution (1 : 3 H_2O_2 : H_2SO_4, which violently reacts with organic compounds and should be used with extreme care) for 30 s to remove organic materials that might be absorbed on the gold electrode surface. The gold electrodes were then rinsed with organic-free water and dried under N_2 in a glove box. The gold electrodes were cycled in 0.5 M H_2SO_4 aqueous solution from −200 mV to 1400 mV vs Ag/AgCl until a stable voltammogram was obtained. Following the cycling, the gold electrodes were rinsed with organic-free water and dried under N_2 again before the self-assembling process.

Electrode modification

The gold electrodes were immersed in 1 mM SAM ethanol solution for 12 h to form a monolayer on the surfaces and rinsed with absolute ethanol to remove any thiol residues on the surface. All the modifications were done at room temperature.

Electrochemical analysis

All experiments were conducted under ambient conditions. The solutions were purged with argon prior to measurements and blanketed with argon during measurements. Peak current i_p was measured as the distance along a vertical line from the peak to the intersection with a baseline that was drawn to intersect tangentially with the curve on either side of the peak.

Results

Figure 1 shows LSV voltammograms of gold electrodes without and with SAM modification (curve A and B respectively) in 1.0 μM $Cu(NO_3)_2$, 0.5 M KNO_3 solution at pH 3.0. The sharp cathodic peak at +50 mV is the reduction peak of Cu^{2+} at a bare gold electrode. The reduction of Cu^{2+} is significantly changed when the gold electrode is modified with 3-mercaptopropionic acid (PA). The reduction peak is broad, and unexpectedly the reduction potential shifts 140 mV positive. This could be the result of some interaction between the self-assembled monolayer and Cu^{2+} ions at the surface.

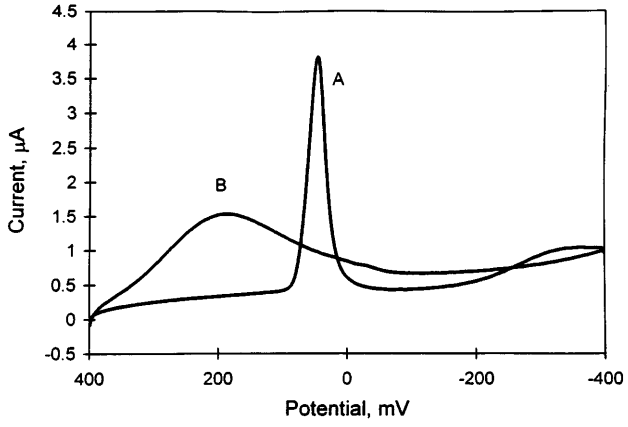

Fig. 1 Linear scan voltammetry (LSV) of 1.0 μM $Cu(NO_3)_2$, 0.5 M KNO_3 (pH 3) at *A* bare gold electrode and *B* SAM-modified gold electrode. SAM: 3-mercaptopropionic acid, 1 mM in ethanol, 12 h immersion. LSV from 400 mV to −400 mV; scan rate 100 mV/s

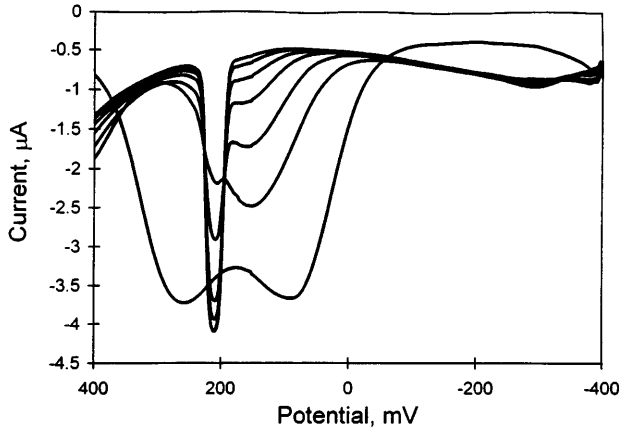

Fig. 3 Deposition time effects on the stripping voltammetry of 1.0 μM $Cu(NO_3)_2$, 0.5 M KNO_3 (pH 3) at bare gold electrode. Osteryoung square wave stripping voltammetry (OSWSV): deposition time: 150 s, 100 s, 50 s, 25 s, 10 s, 5 s, and 1 s; deposition potential: −400 mV; scan from −400 mV to 400 mV; scan rate, 4 mV s^{-1}; SW amplitude, 25 mV; frequency, 14 Hz

When the potential scan is reversed to positive after the negative scan, the copper at the electrode surface will be oxidized, as shown in Fig. 2. The sharp anodic peak in curve A at +240 mV is the oxidation peak of copper at a bare gold electrode. Curve B is the oxidation of copper at the PA-modified gold electrode during the positive scan. There is almost no oxidation peak observed for the modified electrode.

Figure 3 shows stripping voltammograms of oxidation of a copper film formed on deposition in 1.0 μM $Cu(NO_3)_2$, 0.5 M KNO_3 solution at a bare gold electrode at pH 3. The potential was initially held at −400 mV for the deposition of copper onto the electrode surface. For a deposition time of 150 s the anodic peak of copper is split into two peaks at +90 mV and +260 mV respectively, because of the UPD effects. When the deposition time decreases from 150 s to 1 s, there is a dramatic change in the voltammograms. First the peak current at +90 mV decreases while the peak current at +260 mV initially does not change much. After the peak at +90 mV approaches the baseline, the peak at +260 mV starts to decrease as the deposition time decreases. It is clear from this that the peak at +260 mV corresponds to the first monolayer of copper.

When the electrode is modified with PA and used under the same conditions of analysis, the voltammograms changed significantly, as shown in Fig. 4. The twin peaks related to the UPD effects disappeared. There is only one peak at +180 mV in the voltammogram corresponding to the copper oxidation. This peak potential is in between the two oxidation peaks at the bare gold electrode. The charge under the anodic stripping peak is virtually identical to the total charge of both the bulk deposition peak and the monolayer peak for bare gold electrode shown in Fig. 3. The peak is not like the sharp stripping peak at the bare electrode

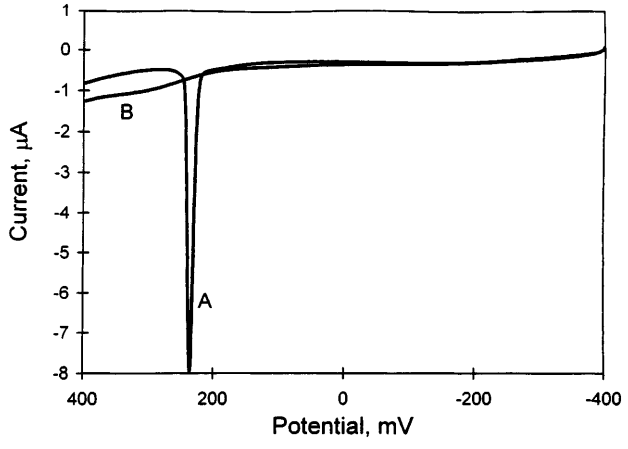

Fig. 2 Linear scan voltammetry (LSV) of 1.0 μM $Cu(NO_3)_2$, 0.5 M KNO_3 (pH 3) at *A* bare gold electrode and *B* SAM-modified gold electrode. SAM: 3-mercaptopropionic acid, 1 mM in ethanol, 12 h immersion. LSV from −400 mV to 400 mV; scan rate 100 mV/s

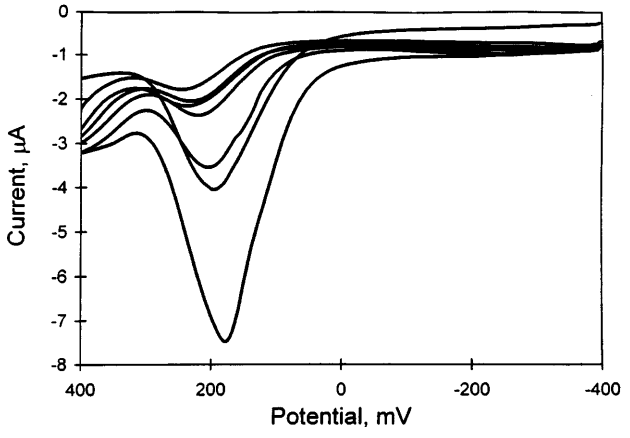

Fig. 4 Deposition time effects on the stripping voltammetry of 1.0 μM $Cu(NO_3)_2$, 0.5 M KNO_3 (pH 3) at SAM-modified gold electrode. SAM: 3-mercaptopropionic acid, 1 mM in ethanol, 12 h immersion. OSWSV settings as per Fig. 3

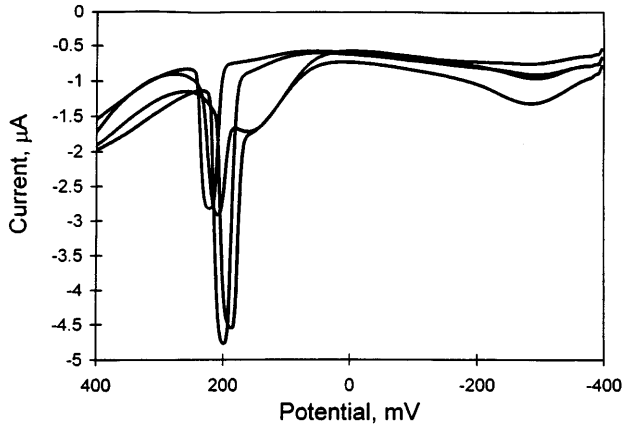

Fig. 5 Concentration effects on the stripping voltammetry of $Cu(NO_3)_2$, 0.5 M KNO_3 (pH 3) at bare gold electrode. $Cu(NO_3)_2$ concentration changes from 1.0 μM to 100 nM, 10 nM, and 1.0 nM. OSWSV: deposition time: 150 s; other settings as per Fig. 3

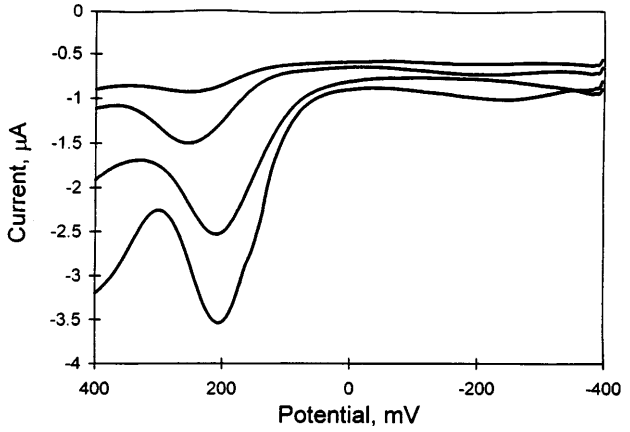

Fig. 6 Concentration effects on the stripping voltammetry of $Cu(NO_3)_2$, 0.5 M KNO_3 (pH 3) at SAM-modified gold electrode. SAM: 3-mercaptopropionic acid, 1 mM in ethanol, 12 h immersion. $Cu(NO_3)_2$ concentration changes from 1.0 μM to 100 nM, 10 nM, and 1.0 nM. OSWSV: deposition time: 150 s; other settings as per Fig. 3

shown in Fig. 3. The peak decreases as the deposition times decreases. Also the peak potential shifts to positive values as the deposition time is lowered. This may indicate that there is an initial interaction between copper and the carboxylate group of the SAM.

Figure 5 shows a Cu^{2+} concentration study at the bare gold electrode. The bulk stripping peak (the more negative peak) current decreases and disappears as the Cu^{2+} concentration decreases from 1.0 μM to 1.0 nM. The monolayer peak potential shifts positively and the peak current decreases as the Cu^{2+} concentration decreases. These peaks are difficult to use for analytical purposes because they are not linear with respect to concentration. After the electrode surface modification with PA, stripping is in the form of a single broad stripping peak, as shown in Fig. 6, which also shifts positively with decreasing Cu^{2+} concentration. Figure 7 shows the calibration curves for Cu^{2+} at both the bare gold electrode and the PA-modified gold electrode. The peak currents are more linear with respect to concentration over a larger range with the SAM modification than either of the two peaks at the bare electrode.

Figure 8 shows OSWV voltammograms for the reduction of $Pb(NO_3)_2$ at gold electrodes without and with SAM modification, curve A and curve B respectively. OSWV was performed at gold electrode in 1.0 μM $Pb(NO_3)_2$, 0.5 M KNO_3 solution at pH 3. At a bare gold electrode the reduction peak potential is −720 mV. When the electrode was modified with PA, the reduction peak current of Pb^{2+} decreases and the peak potential shifts to −810 mV. When the potential scan is reversed the oxidation peaks are shown in Fig. 9.

The results of a deposition time study at a bare gold electrode are shown in Fig. 10. The deposition time decreased from 300 s to 1 s with the deposition potential held at −1000 mV. After the deposition step a positive scan from −1000 mV to 0 mV at the scan rate of 100 mV/s was applied. As expected, two dissolution peaks are observed. The bulk lead stripping peak at

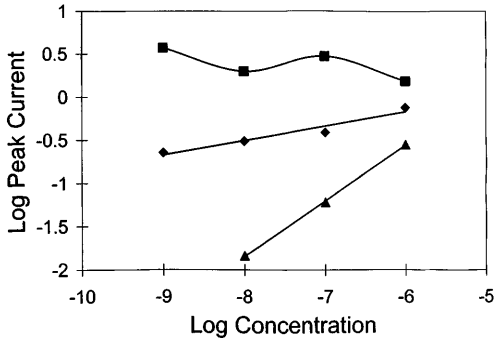

Fig. 7 Calibration curve of $Cu(NO_3)_2$, 0.5 M KNO_3 (pH 3) for (▲) monolayer copper peak, (■) bulk copper peak at a bare gold electrode, and (◆) copper stripping peak at a SAM-modified gold electrode. Conditions as per Fig. 6

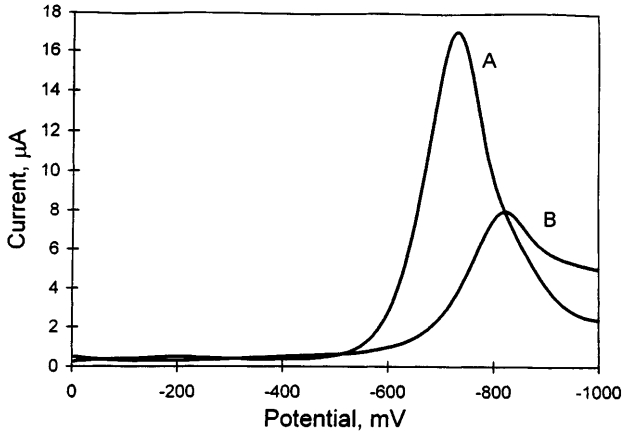

Fig. 8 Osteryoung square-wave voltammetry (OSWV) of 1.0 μM $Pb(NO_3)_2$, 0.5 M KNO_3 (pH 3) at *A* bare gold electrode and *B* SAM-modified gold electrode. SAM: 3-mercaptopropionic acid, 1 mM in ethanol, 12 h immersion. OSWV from 0 mV to −1000 mV; scan rate, 4 mV s^{-1}; SW amplitude, 25 mV; frequency, 14 Hz

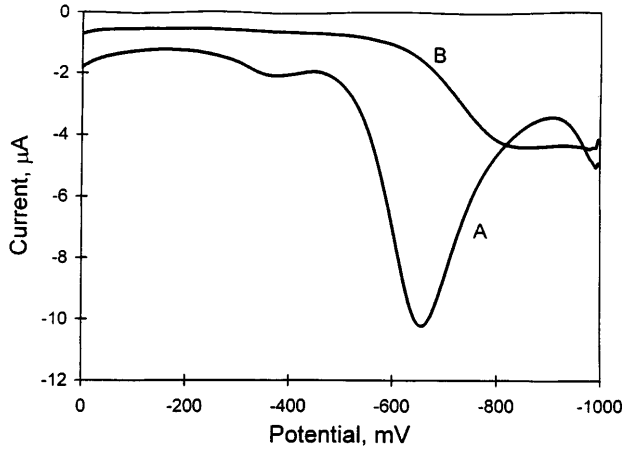

Fig. 9 OSWV of 1.0 μM $Pb(NO_3)_2$, 0.5 M KNO_3 (pH 3) at *A* bare gold electrode and *B* SAM-modified gold electrode. SAM: 3-mercaptopropionic acid, 1 mM in ethanol, 12 h immersion. OSWV from −1000 mV to 0 mV; other settings as per Fig. 8

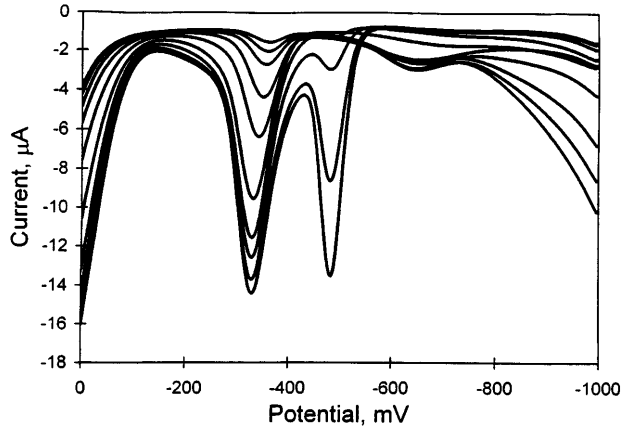

Fig. 10 Deposition time effects on the stripping voltammetry of 1.0 μM $Pb(NO_3)_2$, 0.5 M KNO_3 (pH 3) at bare gold electrode. Osteryoung square-wave stripping voltammetry (OSWSV) deposition time: 300 s, 250 s, 200 s, 150 s, 100 s, 50 s, 25 s, 10 s, 5 s, and 1 s; deposition potential: −1000 mV; scan from −1000 mV to 0 mV; scan rate, 4 mV s^{-1}; SW amplitude, 25 mV; frequency, 14 Hz

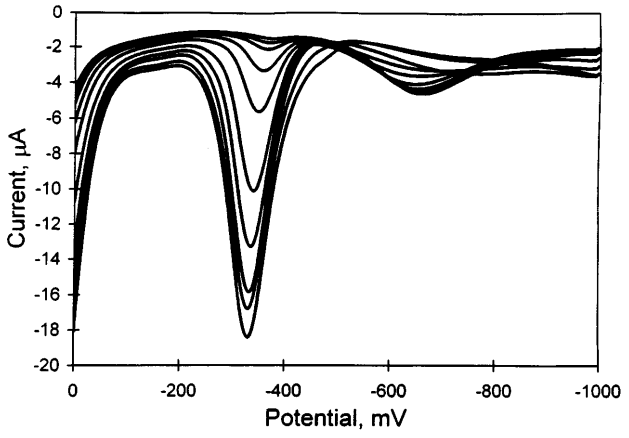

Fig. 11 Deposition time effects on the stripping voltammetry of 1.0 μM $Pb(NO_3)_2$, 0.5 M KNO_3 (pH 3) at SAM-modified gold electrode. SAM: 3-mercaptopropionic acid, 1 mM in ethanol, 12 h immersion. OSWSV settings as per Fig. 10

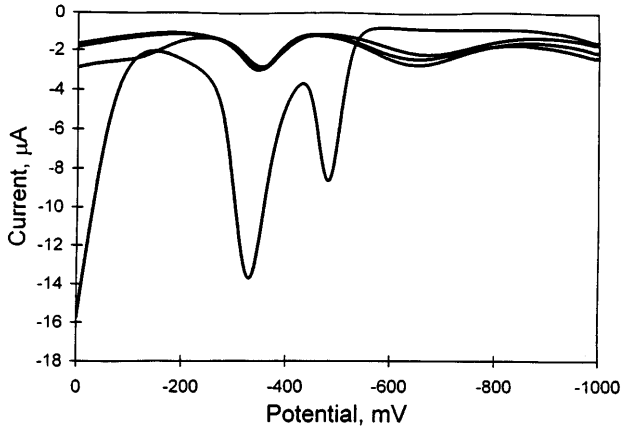

Fig. 12 Concentration effects on the stripping voltammetry of $Pb(NO_3)_2$, 0.5 M KNO_3 (pH 3) at bare gold electrode. $Pb(NO_3)_2$ concentration changes from 1.0 μM to 100 nM, 10 nM, and 1.0 nM. OSWSV deposition time: 250 s; other settings as per Fig. 10

−490 mV decreases as the deposition time decreases and no bulk lead deposition peak is observed when the deposition time is shorter than 100 s. Again the first monolayer of lead being reduced will form stronger intermetallic bonds with gold and shift the monolayer oxidation peak to −320 mV in the positive scan. This UPD peak decreases sharply for a deposition time of less than 100 s. When the electrode is modified with PA, the bulk lead deposition peak is absent and an oxidation peak with a potential of −320 mV is close to the monolayer lead peak potential. As shown in Fig. 11, the peak current decreases with the decreasing deposition time and the peak potential shifts to the negative range when the deposition time decreases.

Figure 12 shows voltammograms of lead oxidation at the bare gold electrode in Pb^{2+} solutions with different concentrations from 1.0 μM to 1.0 nM. The deposition time was held at 150 s for all four experiments. It can be seen that a bulk lead layer forms on the electrode surface during the electrodeposition step of the stripping analysis at higher concentrations (> 1.0 μM). This again results in the twin peaks phenomenon. At lower concentrations there are not sufficient lead ions to form a bulk layer and only the UPD peak is observed. At lower concentrations the monolayer peak remains almost the same for a threefold change of concentration, indicating that this monolayer intermetallic peak is not concentration related and cannot be used for analytical purposes.

The voltammograms for lead solutions of different concentrations at SAM-modified gold electrodes are shown in Fig. 13. Again the bulk lead stripping peak disappears even at higher concentration (1.0 μM). Figure 14 shows the calibration curve of Pb^{2+} at both the bare gold electrode and the PA-modified electrode. The

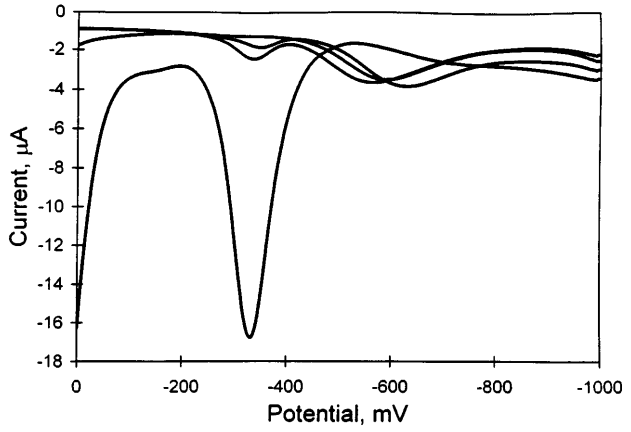

Fig. 13 Concentration effects on the stripping voltammetry of $Pb(NO_3)_2$, 0.5 M KNO_3 (pH 3) at SAM-modified gold electrode. SAM: 3-mercaptopropionic acid, 1 mM in ethanol, 12 h immersion. $Pb(NO_3)_2$ concentration changes from 1.0 μM to 100 nM, 10 nM, and 1.0 nM. OSWSV deposition time: 250 s; other settings as per Fig. 10

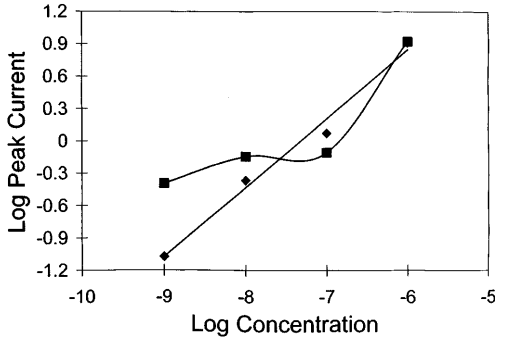

Fig. 14 Calibration curve of $Pb(NO_3)_2$, 0.5 M KNO_3 (pH 3) for (■) bulk lead peak at a bare gold electrode, and (◆) lead stripping peak at a SAM-modified gold electrode. Conditions as per Fig. 13

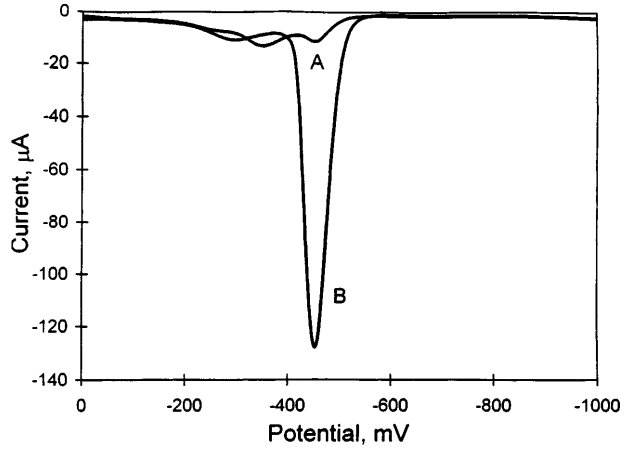

Fig. 15 OSWSV of 1.0 mM $Pb(NO_3)_2$, 0.5 M KNO_3 (pH 7) at *A* bare gold electrode and *B* SAM-modified gold electrode. SAM: 3-mercaptopropionic acid, 1 mM in ethanol, 12 h immersion. OSWSV deposition time: 250 s; other settings as per Fig. 10

lead stripping peak current at −320 mV decreases according to the concentration change when using PA-modified electrodes. The potential shifts to the negative range when the concentration decreases.

The SAMs are terminal carboxylic acids on the electrode surface. When the pH of the solution is higher than 5 (assume pK_a of PA is about 5) these acids will be deprotonated and function as ion exchange sites to electrostatically attract cations like Pb^{2+}. We can take advantage of this to improve the sensitivity of the stripping method. As shown in Fig. 15, voltammogram A is taken in 1 mM Pb^{2+}, 0.5 M KNO_3 solution at bare gold electrode at pH 7. It shows the twin peaks around −400 mV for the oxidation of lead due to the UPD effects. When the gold electrode is modified with PA the peak current increases ten fold, as shown in voltammogram B. The absorption equilibration time is virtually instantaneous. Thus, there is no waiting time period for the preconcentration step with the SAM-modified electrodes.

Repetitive deposition-stripping runs were made on the same SAM-modified electrode. It was found that the first seven to eight cycles were identical with respect to the stripping peaks. Slight changes in peak height and shape occurred, indicating some degradation of the SAM on greater than eight cycles.

Conclusions

Underpotential deposition is a common phenomenon in metal ion anodic stripping analysis at solid electrodes. It is unwanted as the stripping peaks are split and even overlapped in multielement analysis. Also the first monolayer peak is analytically problematic because it is not linearly concentration related. This investigation shows that this problem can be prevented. The self-assembled monolayer using 3-mercaptaopropionic acid as an electrode surface modifier is a promising technique to circumvent the UPD effects during stripping analysis in dilute solutions. The bifunctional thiol also shows its ability to function as an ion exchange site, which could preconcentrate trace cations prior to the electrodeposition step, to enhance sensitivity. The fact that the coulombs for the stripping peaks of the metals at both the SAM-modified electrodes and the bare gold electrodes were essentially identical indicates that the effective electrode surface for deposition is the geometric surface area of the electrode. This suggests that, the deposition is on top of the SAM surface. Also, the fact that the SAM-modified electrode is stable over multiple stripping cycles also suggests that the deposition does not disrupt the SAM film. However, these data do not indicate whether the electron transfers through the SAM film itself or deposition initially occurs at microscopic defects in the SAM film, which fill and then proceed in a three-dimensional manner on the SAM surface.

References

1. Wang J (1990) Anal Chim Acta 234: 41
2. Baldwin RP, Thomsen KN (1991) Talanta 38: 1
3. Wang E, Ji H, Hou W (1991) Electroanalysis 3: 1
4. Sittampalam G, Wilson GS (1983) Anal Chem 55: 1608
5. Wang J, Hutchins LD (1985) Anal Chem 57: 1536
6. Sasso S, Pierce R, Walla R, Yacynych AM (1990) Anal Chem 62: 1111
7. Ji H, Wang E (1987) J Chromatogr 410: 111
8. Shimazu K, Kuwana T (1988) J Electrochem Soc 135: 1602
9. Bremle G, Persson B, Gorton L (1991) Electroanalysis 3: 77
10. Wang J, Golden T, Tuzhi P (1987) Anal Chem 59: 740
11. Wang J, Lu Z (1990) Anal Chem 62: 826
12. Steinberg S, Tor Y, Sabatani E, Rubinstein I (1991) J Am Chem Soc 113: 5176
13. Prime K, Whitesides G (1991) Science 252: 1164
14. Chidsey C, Bertozzi C, Putvinski T, Mujsce A (1990) J Am Chem Soc 112: 4301
15. Tsutsumi H, Furumoto S, Morita M, Matsuda Y (1992) J Electrochem Soc 139: 1522
16. Sun L, Johnson B, Wade T, Crook R (1990) J Phys Chem 94: 8869
17. Collinson M, Bowden E, Tarlov M (1992) Langmuir 8: 1247
18. Shen H, Mark JE, Seliskar CJ, Mark HB Jr, Heineman WR (1997) J Solid State Electrochem (in press)
19. Malem F, Mandler D (1993) Anal Chem 65: 37
20. Porter M, Bright T, Allara D, Chidsey CED (1987) J Am Chem Soc 109: 3559
21. Kuhn HJ (1979) Photochem 10: 111
22. Polymeropoulos EE, Möbius D, Kuhn H (1980) Thin Solid Films 68: 173
23. Fromherz P, Arden W (1980) J Am Chem Soc 102: 6211
24. Lehn JM (1985) Science 227: 849
25. Arrhenius TS, Blanchard-Desce M, Dvolaitzky M, Lehn JM, Malthete J (1986) Proc Nat Acad Sci USA 83: 5355
26. Kumano A, Niwa O, Kajiyama T, Takayanagi M, Kunitake T (1984) Polymer J 16: 461
27. Ringsdorf H, Schmidt G, Schneider J (1987) Thin Solid Films 152: 207
28. Proc 2nd Int Conf on Langmuir-Blodgett Films, Schenectady (1985) Thin Solid Films 132: 1
29. Fendler JH (1987) J Membrane Sci 30: 323
30. Steingerg S, Rubinstein I (1992) Langmuir 8: 1183
31. Cheng Q, Brajter-Toth A (1992) Anal Chem 64: 1998
32. Yip CM, Ward MD (1994) Langmuir 10: 549
33. Sun L, Johnson B, Wade T, Crooks RM (1990) J Phys Chem 94: 8869
34. Wulff G, Heide B, Helfmeier, G (1986) J Am Chem Soc 108: 1089
35. Heckl WM, Marassi FM, Kallury KMR, Stone DC, Thompson M (1990) Anal Chem 62: 32
36. Kepley LJ, Crooks RM, Ricco AJ (1992) Anal Chem 64: 3192
37. Steinberg S, Tor Y, Sabatani E, Rubinstein I (1991) J Am Chem Soc 113: 5176
38. Bard AJ, Faulkner LR (1980) Electrochemical methods: fundamentals and applications. John Wiley, New York
39. Nikelly JG, Cooke WD (1957) Anal Chem 29: 933
40. De-Mars RD, Shain I (1957) Anal Chem 29: 1825
41. Kemula W, Kublik Z (1958) Anal Chim Acta 18: 104
42. Nicholson MM (1960) Anal Chim Acta 32: 1058
43. Nicholson MM (1957) J Am Chem Soc 79: 7
44. Bryne JT, Rogers LB, Griess JC Jr (1951) J Electrochem Soc 98: 452
45. Rogers LB, Krause DP, Griess JC Jr, Ehrlinger DB (1949) J Electrochem Soc 95: 33